

# Analysis of Temperature and Concentration Polarizations to Improve the Performance of Vacuum Membrane Distillation

Junfeng Zhu<sup>1</sup>, Xingtian Wang<sup>1</sup>, Yingjie Wu<sup>1</sup>, Junkui Niu<sup>1</sup>, Danping Wang<sup>2</sup>, Shiwen Hou<sup>1</sup>

<sup>1</sup>Institute of Pastoral Hydraulic Research, Hohhot, China

<sup>2</sup>Hohhot Meteorological Bureau, Hohhot, China

Email: mansub2007@163.com

**How to cite this paper:** Zhu, J. F., Wang, X. T., Wu, Y. J., Niu, J. K., Wang, D. P., & Hou, S. W. (2024). Analysis of Temperature and Concentration Polarizations to Improve the Performance of Vacuum Membrane Distillation. *Journal of Geoscience and Environment Protection*, 12, 272-283.  
<https://doi.org/10.4236/gep.2024.1211015>

**Received:** October 28, 2024

**Accepted:** November 26, 2024

**Published:** November 29, 2024

Copyright © 2024 by author(s) and Scientific Research Publishing Inc. This work is licensed under the Creative Commons Attribution International License (CC BY 4.0).  
<http://creativecommons.org/licenses/by/4.0/>



Open Access

## Abstract

Vacuum membrane distillation technology shows considerable promise for the treatment of mine water. Nevertheless, the current vacuum membrane distillation technology's significant reliance on a heat source presents a challenging equilibrium between its energy consumption and thermal efficiency. Consequently, the present study employed computational fluid dynamics (CFD) calculations and analyses to examine the phenomena of temperature-differential polarisation and concentration-differential polarisation generated during the membrane distillation process, and to ascertain the extent to which the operating parameters affect them. Furthermore, it was observed that CPC and TPC exhibited a notable decline with the elevation of feed inlet temperature, while the polarisation phenomenon was diminished with the augmentation of feed inlet flow rate. The optimal equilibrium between membrane flux and thermal efficiency is intimately associated with the operating parameters. Additionally, this study offers a theoretical rationale for the enhancement of vacuum membrane distillation performance.

## Keywords

Vacuum Membrane, Temperature Polarization, Concentration Polarization, Hollow Fibre, Membrane Flux

## 1. Introduction

In recent years, membrane distillation (MD), a novel heat-driven membrane technology, has demonstrated promising potential for application in the field of industrial wastewater treatment (Qasim et al., 2021). This is due to a number of

factors, including its mild operating conditions, high water yield, effective separation performance, and capacity to utilise industrial waste heat. In comparison to conventional pressure-driven membrane technologies, such as nanofiltration and reverse osmosis, membrane distillation does not necessitate a high-quality input of raw water (Wan Osman et al., 2021). It is capable of producing a high-quality output of treated water when processing wastewater with a high concentration of recalcitrant compounds (Chamani et al., 2021). This technology has been successfully employed in the treatment of typical industrial wastewater (Zheng et al., 2023).

The phenomenon of differential temperature polarisation is of great significance in the field of membrane distillation technology, as it has a direct impact on the efficiency and energy consumption of the membrane distillation process. In particular, the phenomenon of differential temperature polarisation is a significant issue in the context of membrane distillation, as it can result in a reduction in driving force, a decline in permeate flux and an increase in energy consumption (Lu et al., 2019). The underlying cause of this phenomenon can be attributed to the necessity for significant heat absorption during membrane distillation, due to the evaporation of the feed solution on the membrane surface (Anvari et al., 2020). This results in a reduction in the temperature at the membrane surface, below the body temperature, thereby diminishing the actual driving force. The temperature difference is of critical importance as a driving force for separation. The generation of temperature polarisation has the effect of weakening this driving force, thus affecting the performance of membrane distillation (Zhang & Guo, 2024).

The study of differential temperature polarisation is a crucial aspect of optimising membrane distillation technology, as it enables a deeper understanding of and potential improvements to the efficiency of heat and mass transfer in membrane distillation processes. By analysing the effect of feed liquid flow rate and membrane properties on differential temperature polarisation, measures can be taken to mitigate this phenomenon. These include optimising membrane module design, using modified membranes, applying external physical fields, etc., with the aim of increasing membrane flux or reducing membrane contamination. In addition, the development of composite membranes with thermal conductivity to heat the cold feed is expected to significantly reduce the differential temperature polarisation at the source and improve the membrane distillation performance.

In previous numerical studies of vacuum membrane distillation processes, the concentration variation of the feed solution during membrane distillation has not been considered. This has implications for the partial vapour pressure difference and, consequently, the transmembrane mass flux. In order to address these issues, the present study combines substance transfer and concentration variations to obtain water production, thermal efficiency and power consumption. This approach is designed to enhance the potential of vacuum membrane distillation performance.

## 2. Theory and Modelling

The membrane distillation process is illustrated in **Figure 1**. The feed solution is subjected to heating and circulation on the feed side. The hollow fibre membrane is a hydrophobic PTFE selective permeable membrane. The water vapour traverses the membrane and subsequently, following its transportation to the vacuum side by the vacuum pump, enters the condenser. Thereafter, the water is reused in the form of distilled water.

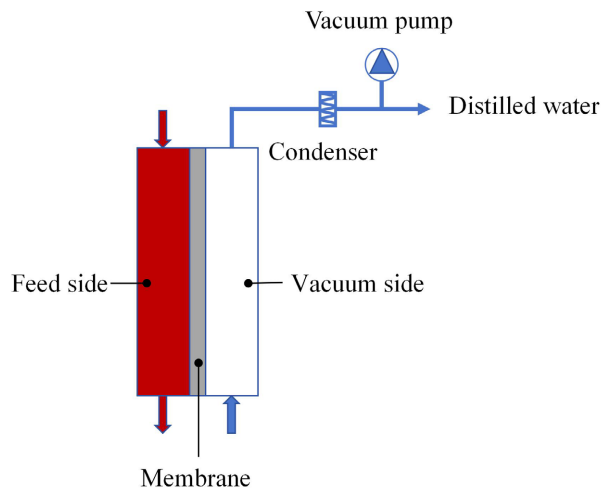


**Figure 1.** Vacuum membrane distillation process.

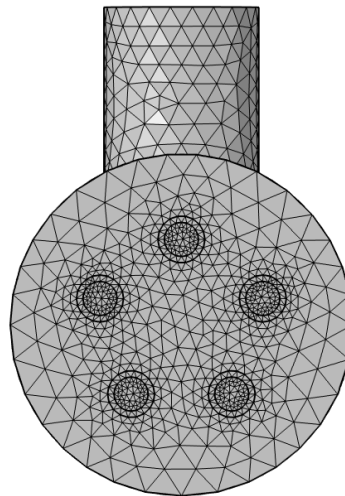


**Figure 2.** Grids generated for the computation domain for the configuration.

To further investigate the effects of temperature difference and concentration polarisation on thermal efficiency and membrane flux, the membrane grid was divided into a more finely-meshed configuration, as illustrated in **Figure 2**. The hollow fibre membranes were composed of PTFE medium control fibre membranes with an average pore size of  $0.16 \mu\text{m}$  and a porosity of 85%, with an inner diameter of 0.8 mm and an outer diameter of 1.1 mm. The total number of

membranes was five lengths of 400 mm. The overall dimensions of the VMD module were 8 mm (diameter) × 400 mm (length). The impact of varying feed concentration compositions was investigated, with distilled water at salinities of 15 - 90 g/kg prepared with NaCl. The feed inlet temperature ranged from 40 to 80 degrees Celsius, the volumetric flow rate was 0.6 L/min, and the permeate vacuum pressure was set at 5 kPa. The experimental conditions are summarised in **Table 1**.

**Table 1.** Geometry specifications and experimental conditions of the model.

Hollow fiber vacuum membrane module	Value
Effective length of fiber (mm)	400
Shell diameter (mm)	8
Amount of fibers	5
Inner diameter of fiber (mm)	0.8
Outer diameter of fiber (mm)	1.1
Porosity (%)	85
Mean pore diameter (μm)	0.16
Feed pressure (kPa)	350
Feed salinity (g/kg)	45
Feed inlet flow rate (m/s)	0.6
Vacuum pressure (kPa)	50
Feed inlet temperature (K)	313.15 - 353.155

### 3. Theoretical Modelling and Validation

#### 3.1. Heat Transfer Model

During the VMD process, the permeate side region of the membrane is always in a high vacuum environment and the membrane material itself has poor thermal conductivity, so the heat loss is generally ignored in the modelling process. According to the principle of energy conservation, the following equation can be obtained (Xu et al., 2009):

$$Q_b = Q_m \quad (1)$$

where  $Q_b$  is the heat of the feed liquid and  $Q_m$  is the latent heat of evaporation transfer.

The heat and latent heat of vapour transferred between the membrane surface and the feed liquid is calculated using the following equation (Shakaib et al., 2011):

$$Q_b = h_f (T_f - T_{fm}) \quad (2)$$

$$Q_m = N\Delta H_v + \frac{K_m}{\delta} (T_{fm} - T_{pm}) \quad (3)$$

where  $\delta$  is the membrane thickness (m),  $T_{fm}$  is the temperature of the

membrane surface on the feed side (K),  $T_{pm}$  is the temperature of the membrane surface on the permeate side (K),  $N$  is the membrane flux per unit time ( $\text{kg}\cdot\text{m}^{-2}\cdot\text{h}^{-1}$ ), and the equation of the relationship between the temperature of the membrane surface and the latent heat of vapour is as follows (Hasani et al., 2019):

$$\Delta H_v = 2489.7 - 2.412(T_{fm} - 278.15) \quad (4)$$

In the existing research literature, the calculation of heat transfer coefficients is based on the Nussell number. Although the models used in the various studies are different, the theory and procedure are basically the same. Based on these empirical formulas, the following Nussell's formula can be derived (Shokrollahi et al., 2020):

$$N_u = \frac{h_f \cdot d}{k} \quad (5)$$

where  $d$  is the film thickness (m) and  $k$  is the thermal conductivity ( $\text{W}\cdot\text{m}^{-1}\cdot\text{K}^{-1}$ ).

Local heat transfer coefficient and the temperature polarization coefficient (TPC) are as follows (Abrofarakh et al., 2024) (Yao et al., 2023):

$$h_f = \frac{Q_b}{T_f - T_{fm}} = \frac{Q_m}{T_f - T_{fm}} \quad (6)$$

$$\text{TPC} = \frac{T_{fm}}{T_f} \quad (7)$$

The thermal efficiency of VMD can be expressed (Vanneste et al., 2017):

$$\eta = \frac{J \Delta H_v}{V_f C_p \Delta T_f} \quad (8)$$

where  $V_f$  and  $\Delta T_f$  are feed velocity and temperature drop along with the fiber, respectively.

### 3.2. Mass Transfer Model

In membrane distillation operation, material transfer and heat transfer are inter-related processes. Thus, the membrane flux of VMD can be calculated by the following equation (Abrofarakh et al., 2024):

$$H = K_m \cdot p = K_m \cdot (P_1 - P_2) \quad (9)$$

where  $P_1$  is the membrane surface pressure (Pa) on the feed side and  $P_2$  is the membrane surface pressure (Pa) on the permeate side.

On this basis, three main mass transfer mechanisms were proposed: molecular diffusion, Knudsen diffusion and viscous flow. In VMD, due to the negative pressure on the cold side, there is only a small amount of water vapour in the pore space of the membrane, and the resistance caused by the collision between molecules is negligible, and the driving force for the transfer is the saturated vapour pressure on the inlet side and the absolute pressure difference on the permeate side. The Knudsen number ( $K_n$ ) is (Soukane et al., 2017; Zare &

Kargari, 2022):

$$K_n = \frac{\lambda}{d} \quad (10)$$

where  $\lambda$  is the mean free range of water vapour (m) and  $d$  is the mean pore diameter of the membrane (m).

The calculated expression for the mean free range of water vapour through the membrane is as follows (Choi et al., 2024):

$$\lambda = \frac{K_b T}{\sqrt{2\pi P d_1^2}} \quad (11)$$

where  $K_b$  has a value of  $1.38 \times 10^{-23} \text{ J}\cdot\text{K}^{-1}$  and  $d_1$  is the collision diameter value of  $2.641 \times 10^{-10} \text{ m}$ . The mass transfer mechanism in this study is a viscous flow-Nussén diffuser.

The mass transfer mechanism in this study is a viscous flow-Nussén diffusion machine, so the equation for the transmembrane mass transfer flux is (Lou et al., 2022):

$$N = (C_1 + C_2) \Delta P \quad (12)$$

where  $C_1$  is the viscous flow coefficient,  $C_2$  is the Knudsen coefficient, and  $\Delta P$  is the vapour partial pressure difference.

The concentration polarization coefficient (CPC) is as follows (Lokare & Vidic, 2019):

$$\text{CPC} = \frac{C_{fm}}{C_f} \quad (13)$$

$C_{fm}$  is the concentration of the solution on the surface of the distillation membrane, and  $C_f$  is the concentration of the main body of the solution.

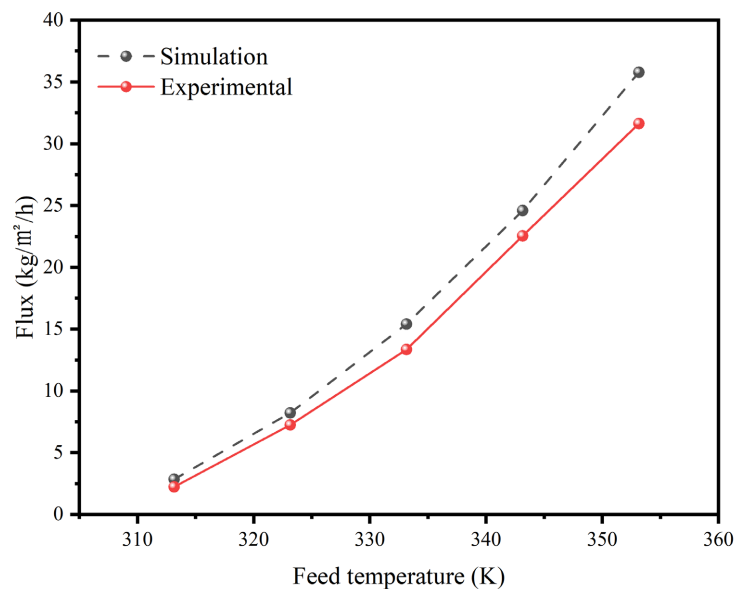


**Figure 3.** Experimental and simulation comparison (feed flow rate = 0.45 m/s; salinity = 4.5%; vacuum side pressure = -5 kPa).

### 3.3. Model Validation

**Figure 3** illustrates the comparison between the experimental data and the simulated results of the flux of the vacuum fibre membrane distillation module based on different feed temperatures (313, 323, 333, 343, 353 K). The calculated error values demonstrate that the simulated and experimental data exhibit a satisfactory agreement at different feed temperatures.

## 4. Results and Discussion

### 4.1. Concentration Polarization Coefficient

As illustrated in **Figure 4**, the concentration polarisation factor demonstrates minimal variation with increasing salinity of the feed solution. Furthermore, an increase in the inlet flow rate of the feed solution results in a reduction in polarization. The gradient rate of change of CPC with feed liquid inlet velocity is 0.95, 0.42, 0.24, 0.26, indicating that when the inlet flow rate reaches 0.45 m/s, there is a notable improvement in concentration polarisation. Furthermore, the change in concentration polarisation with the increase in inlet flow rate begins to plateau.

It can be seen in **Figure 5** that the concentration polarisation coefficient exhibits a notable decline with rising feed inlet temperature. This is attributed to the fact that elevated temperatures enhance the water vapour flux at the membrane interface, thereby exhibiting a more pronounced concentration polarisation (Darman et al., 2023). Consequently, as temperature increases, the membrane flux also rises. However, the accompanying surge in energy consumption is a significant concern that will be elaborated upon in the thermal efficiency section.

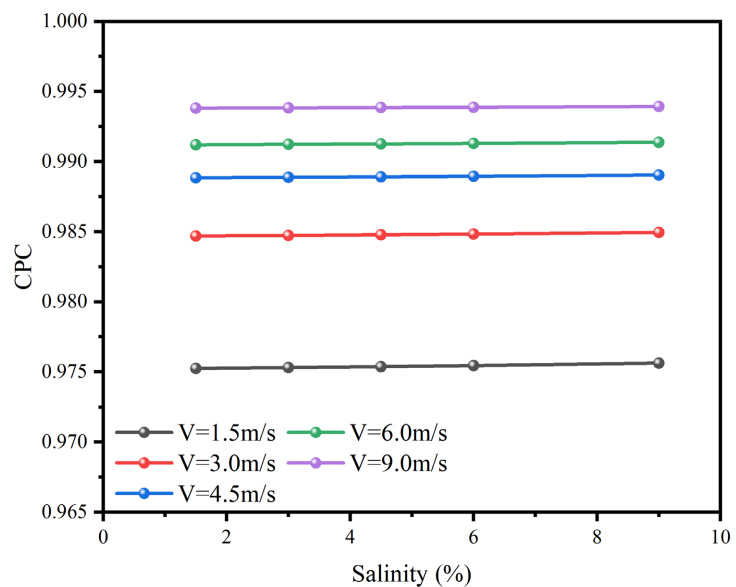


**Figure 4.** Concentration polarization coefficient along the salinity under the feed inlet temperature at 343.15 K.

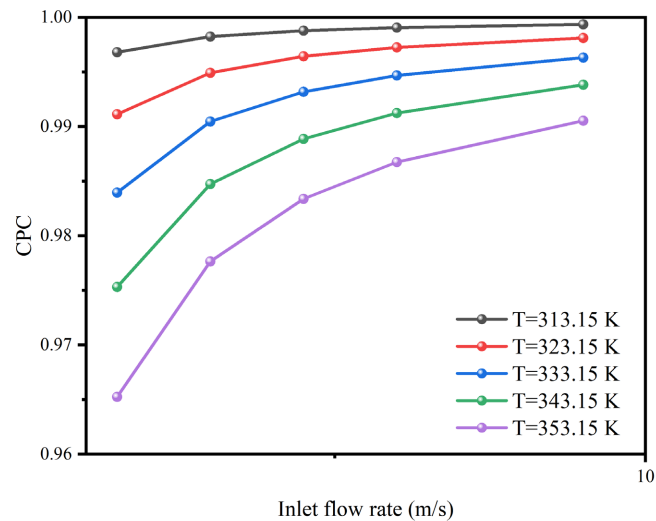


**Figure 5.** Concentration polarization coefficient along the feed inlet flow rate under the feed salinity at 3%.

#### 4.2. Temperature Polarization Coefficient

**Figure 6** displays the trend of the temperature polarisation coefficient as a function of the inlet temperature. It is evident that the inlet and outlet temperatures exert a considerable influence on the TPC. As the temperature rises, the temperature gradient of the feed solution in the hollow fibre membrane tube becomes markedly more pronounced. Furthermore, temperature polarisation results in an uneven heat transfer, which ultimately leads to a reduction in thermal efficiency. Achieving an optimal balance between thermal efficiency and membrane flux can further enhance the efficiency of vacuum membrane distillation (Andrés-Mañás et al., 2023). Increasing the inlet flow rate can mitigate the impact of temperature polarisation and improve thermal efficiency.

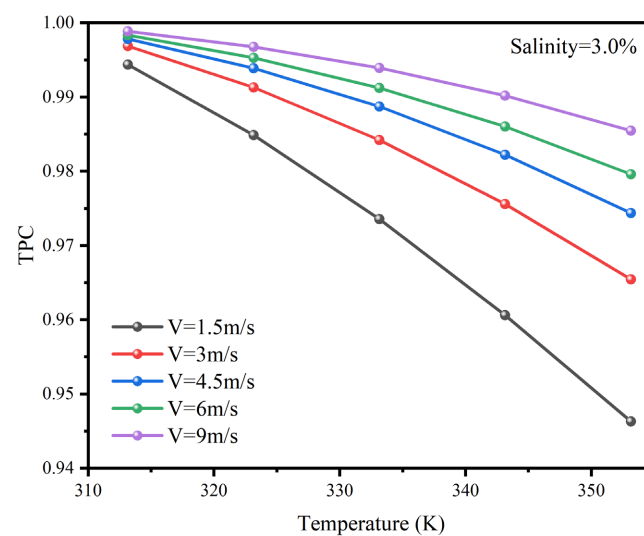


**Figure 6.** Temperature polarization coefficient along the feed inlet temperature under the feed salinity at 3%.

### 4.3. Thermal Efficiency

Figure 7 presents a plot of thermal efficiency as a function of temperature and flow rate. It is evident that an increase in the inlet flow velocity has a considerable impact on the thermal efficiency. However, the improvement in thermal efficiency brought about by an increase in the inlet velocity to 0.45 m/s is less pronounced. As the temperature rises, the decline in thermal efficiency becomes less steep, occurring between 323.15 and 343.15 K. Consequently, a more detailed examination of the efficiency of vacuum membrane distillation in conjunction with membrane flux is crucial.

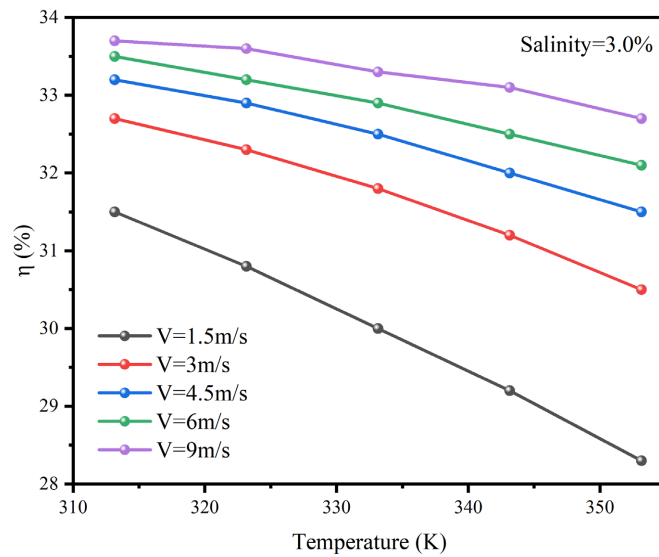


Figure 7. Thermal efficiency distribution along the along the feed inlet temperature under the feed salinity at 3%.

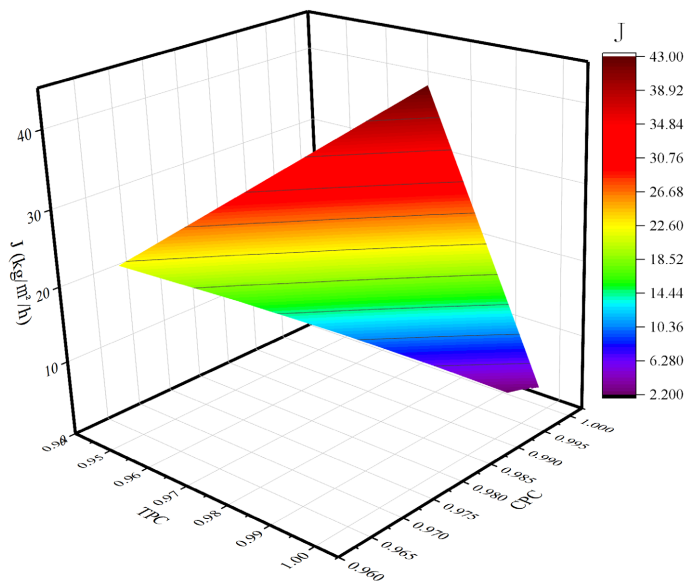


Figure 8. Surface plots of temperature polarisation coefficient and concentration polarisation coefficient versus membrane flux.

#### 4.4. Overall Performance

**Figure 8** provides a visual representation of the relationship between TPC and CPC and membrane flux. At TPC = 0.985 and CPC = 0.990, the membrane flux is observed to reach  $42 \text{ kg}\cdot\text{m}^{-2}\cdot\text{h}^{-1}$ . In light of the aforementioned results, it can be concluded that a high level of thermal efficiency is achieved at an inlet flow rate of 0.45 m/s and an inlet temperature within the range of 323.15 to 343.15 K. Consequently, the optimal operating parameters between thermal efficiency and membrane flux must be identified on the basis of the cost of energy supply.

#### 5. Conclusion

This study investigates the results of the temperature polarisation coefficient, concentration polarisation coefficient, thermal efficiency and membrane flux based on CFD simulations. It was observed that there was a notable decline in CPC and TPC with the rise in feed inlet temperature, and that the polarisation was diminished with the increase in feed inlet flow rate. Conversely, thermal efficiency demonstrated a negative correlation with feed inlet temperature. The optimal equilibrium between membrane flux and thermal efficiency is closely associated with the operating parameters. This study also provides further insight into the impact of polarisation coefficient on the performance of vacuum membrane distillation.

#### Acknowledgements

This work was supported by the Key special projects of the “Science and Technology for the Development of Inner Mongolia” initiative (2022EEDSKJXMO04) and Science and Technology Plan Program of Inner Mongolia Autonomous Region (2022YFHH0100).

#### Conflicts of Interest

The authors declare no conflicts of interest regarding the publication of this paper.

#### References

- Abrofarakh, M., Moghadam, H., & Abdulrahim, H. K. (2024). Investigation of Direct Contact Membrane Distillation (DCMD) Performance Using CFD and Machine Learning Approaches. *Chemosphere*, 357, Article ID: 141969. <https://doi.org/10.1016/j.chemosphere.2024.141969>
- Andrés-Mañas, J. A., Requena, I., & Zaragoza, G. (2023). Membrane Distillation of High Salinity Feeds: Steady-State Modelling and Optimization of a Pilot-Scale Module in Vacuum-Assisted Air Gap Operation. *Desalination*, 553, Article ID: 116449. <https://doi.org/10.1016/j.desal.2023.116449>
- Anvari, A., Azimi Yancheshme, A., Kekre, K. M., & Ronen, A. (2020). State-of-the-Art Methods for Overcoming Temperature Polarization in Membrane Distillation Process: A Review. *Journal of Membrane Science*, 616, Article ID: 118413. <https://doi.org/10.1016/j.memsci.2020.118413>
- Chamani, H., Woloszyn, J., Matsuura, T., Rana, D., & Lan, C. Q. (2021). Pore Wetting in

- Membrane Distillation: A Comprehensive Review. *Progress in Materials Science*, 122, Article ID: 100843. <https://doi.org/10.1016/j.pmatsci.2021.100843>
- Choi, J., Cho, J., Cha, H., & Song, K. G. (2024). Computational Fluid Dynamics Simulation of the Stacked Module in Air Gap Membrane Distillation for Enhanced Permeate Flux and Energy Efficiency. *Applied Energy*, 360, Article ID: 122805. <https://doi.org/10.1016/j.apenergy.2024.122805>
- Darman, M., Niknafs, N., & Jalali, A. (2023). Effect of Wavy Corrugations on the Performance Enhancement of Direct Contact Membrane Distillation Modules: A Numerical Study. *Chemical Engineering and Processing—Process Intensification*, 190, Article ID: 109421. <https://doi.org/10.1016/j.cep.2023.109421>
- Hasani, S. M. F., Sowayan, A. S., & Shakaib, M. (2019). The Effect of Spacer Orientations on Temperature Polarization in a Direct Contact Membrane Distillation Process Using 3-D CFD Modeling. *Arabian Journal for Science and Engineering*, 44, 10269-10284. <https://doi.org/10.1007/s13369-019-04089-x>
- Lokare, O. R., & Vidic, R. D. (2019). Impact of Operating Conditions on Measured and Predicted Concentration Polarization in Membrane Distillation. *Environmental Science & Technology*, 53, 11869-11876. <https://doi.org/10.1021/acs.est.9b04182>
- Lou, J., Dudley, M., Wang, J., Liu, Y., Cath, T. Y., Turchi, C. S. et al. (2022). Numerical Simulations of Membrane Distillation Systems with Actively Heated Membranes. *Journal of Membrane Science*, 668, Article ID: 121206. <https://doi.org/10.1016/j.memsci.2022.121206>
- Lu, K. J., Chen, Y., & Chung, T. (2019). Design of Omniphobic Interfaces for Membrane Distillation—A Review. *Water Research*, 162, 64-77. <https://doi.org/10.1016/j.watres.2019.06.056>
- Qasim, M., Samad, I. U., Darwish, N. A., & Hilal, N. (2021). Comprehensive Review of Membrane Design and Synthesis for Membrane Distillation. *Desalination*, 518, Article ID: 115168. <https://doi.org/10.1016/j.desal.2021.115168>
- Shakaib, M., Hasani, S. M. F., Ahmed, I., & Yunus, R. M. (2011). A CFD Study on the Effect of Spacer Orientation on Temperature Polarization in Membrane Distillation Modules. *Desalination*, 284, 332-340. <https://doi.org/10.1016/j.desal.2011.09.020>
- Shokrollahi, M., Rezakazemi, M., & Younas, M. (2020). Producing Water from Saline Streams Using Membrane Distillation: Modeling and Optimization Using CFD and Design Expert. *International Journal of Energy Research*, 44, 8841-8853. <https://doi.org/10.1002/er.5578>
- Soukane, S., Naceur, M. W., Francis, L., Alsaadi, A., & Ghaffour, N. (2017). Effect of Feed Flow Pattern on the Distribution of Permeate Fluxes in Desalination by Direct Contact Membrane Distillation. *Desalination*, 418, 43-59. <https://doi.org/10.1016/j.desal.2017.05.028>
- Vanneste, J., Bush, J. A., Hickenbottom, K. L., Marks, C. A., Jassby, D., Turchi, C. S. et al. (2017). Novel Thermal Efficiency-Based Model for Determination of Thermal Conductivity of Membrane Distillation Membranes. *Journal of Membrane Science*, 548, 298-308. <https://doi.org/10.1016/j.memsci.2017.11.028>
- Wan Osman, W. N. A., Mat Nawi, N. I., Samsuri, S., Bilad, M. R., Wibisono, Y., Hernández Yáñez, E. et al. (2021). A Review on Recent Progress in Membrane Distillation Crystallization. *ChemBioEng Reviews*, 9, 93-109. <https://doi.org/10.1002/cben.202100034>
- Xu, Z., Pan, Y., & Yu, Y. (2009). CFD Simulation on Membrane Distillation of NaCl Solution. *Frontiers of Chemical Engineering in China*, 3, 293-297. <https://doi.org/10.1007/s11705-009-0204-7>

- Yao, Y., Yu, S., & Battiato, I. (2023). Understanding Flow Dynamics in Membrane Distillation: Effects of Reactor Design on Polarization. *Separation and Purification Technology*, 314, Article ID: 123664. <https://doi.org/10.1016/j.seppur.2023.123664>
- Zare, S., & Kargari, A. (2022). CFD Simulation and Optimization of an Energy-Efficient Direct Contact Membrane Distillation (DCMD) Desalination System. *Chemical Engineering Research and Design*, 188, 655-667. <https://doi.org/10.1016/j.cherd.2022.10.001>
- Zhang, Y., & Guo, F. (2024). Mitigating Near-Surface Polarizations in Membrane Distillation via Membrane Surface Decoration. *Desalination*, 579, Article ID: 117507. <https://doi.org/10.1016/j.desal.2024.117507>
- Zheng, L., Li, C., Zhang, C., Kang, S., Gao, R., Wang, J. et al. (2023). Mixed Scaling Deconstruction in Vacuum Membrane Distillation for Desulfurization Wastewater Treatment by a Cascade Strategy. *Water Research*, 238, Article ID: 120032. <https://doi.org/10.1016/j.watres.2023.120032>